

VisioPhysioENet: Multimodal Engagement Detection using Visual and Physiological Signals

Alakhsimar Singh^{*†}, Nischay Verma^{*†}, Kanav Goyal^{*†}, Amritpal Singh^{#†}, Puneet Kumar[‡], Xiaobai Li^{§†}

[†]Computer Science and Engineering Department, National Institute of Technology, Jalandhar, India

[‡]Center for Machine Vision and Signal Analysis, University of Oulu, Finland

[§]The State Key Laboratory of Blockchain and Data Security, Zhejiang University, Hangzhou, China

Abstract—This paper presents VisioPhysioENet, a novel multimodal system that leverages visual and physiological signals to detect learner engagement. It employs a two-level approach for extracting both visual and physiological features. For visual feature extraction, Dlib is used to detect facial landmarks, while OpenCV provides additional estimations. The face_recognition library, built on Dlib, is used to identify the facial region of interest specifically for physiological signal extraction. Physiological signals are then extracted using the plane-orthogonal-to-skin method to assess cardiovascular activity. These features are integrated using advanced machine learning classifiers, enhancing the detection of various levels of engagement. We thoroughly tested VisioPhysioENet on the DAiSEE dataset. It achieved an accuracy of 63.09%. This shows it can better identify different levels of engagement compared to many existing methods. It performed 8.6% better than the only other model that uses both physiological and visual features.

Index Terms—Student Engagement Analysis, Online Learning, Multimodal Fusion, Visual Features, rPPG Signals.

I. INTRODUCTION

Engagement detection in educational settings is essential for optimizing learning outcomes [1]. Traditional methods, often limited by their reliance on a single data type, may not fully capture the complexities of learner engagement [2], [3]. Recent studies advocate for multimodal engagement detection, which integrates various data types to overcome the limitations of unimodal approaches [4], [5]. Although these multimodal systems combining visual and physiological signals show improved accuracy and comprehensiveness [6], [7], they still face challenges such as data imbalance and limited generalizability across different datasets [8], [9]. Additionally, most of the research in this domain has predominantly focused on visual data, with little emphasis on exploiting multimodality [2]. VisioPhysioENet utilizes a multimodal approach to uncover subtle patterns of disengagement, enabling precise interventions like adapting instructional methods. This strategy enhances learning and provides educators with tools for meaningful academic success.

The proposed multimodal engagement detection framework, VisioPhysioENet, addresses these challenges by leveraging advanced machine learning algorithms and multimodal data integration. This ensures a balance between accuracy and computational efficiency, avoiding the complexities of deep

neural architectures [9], [10]. The system employs a two-level approach for visual and physiological feature extraction. First, using Dlib [11] to extract facial landmarks, and OpenCV [12] for eye and head metrics like Eye Aspect Ratio (EAR), Pitch, Yaw, and Roll. These are transformed into numerical features and categorized into actionable classes, including eye openness, gaze direction, and head position. In parallel, remote photoplethysmography (rPPG) signals [13] are captured from video input to monitor cardiovascular activity. The rPPG method utilizes the face_recognition [14] library, which incorporates Dlib, to identify and extract the region of interest (ROI) for processing. These extracted signals are then further analyzed to compute meaningful metrics, such as heart rate, average peak-to-peak interval time, cumulative sum of systolic peaks, and cumulative sum of diastolic peaks.

Transitioning from the initial processing of time-serialized signals to handling single-value data points in the final phase, VisioPhysioENet significantly reduces computational demands and enhances system robustness. This integration of visual and physiological data through advanced machine learning models, specifically multi-output classifiers, and the application of late fusion techniques ensures improved accuracy and robustness in detecting engagement levels. When rigorously evaluated on the Dataset for Affective States in E-Environments (DAiSEE) dataset [15], VisioPhysioENet achieves an accuracy of 63.09%, demonstrating a superior ability to discern various levels of engagement compared to existing methodologies. The major contributions of this paper are listed as follows:

- Proposal for VisioPhysioENet, a framework that integrates physiological information with visual data, eliminating the need for additional measurement devices while delivering a lightweight, fast, and computationally efficient solution.
- Implementation of multimodal fusion techniques, including early and late fusion strategies, to integrate visual and physiological data for robust engagement detection.
- Rigorous validation on the DAiSEE dataset, with detailed ablation studies that highlight improvements over existing methods, contributing significantly to the field.

II. RELATED WORKS

The detection and analysis of learner engagement have advanced significantly, progressing from single-modal approaches to sophisticated multimodal systems. These methods

* denotes equal contribution # denotes corresponding author

aim to tackle the complexities of engagement detection in dynamic, real-world scenarios.

Initial works focused on single data modalities, such as visual or physiological signals. Abedi et al. [6] employed ResNet with temporal convolutional networks to extract spatiotemporal features from video datasets like DAiSEE. This approach highlighted the value of leveraging temporal patterns for engagement detection. Similarly, Selim et al. [7] utilized EfficientNet combined with Long Short-Term Memory (LSTM) networks for video-based engagement detection, showcasing the effectiveness of sequential modelling. However, their efforts were constrained by imbalanced datasets, a recurring challenge in engagement research.

The integration of physiological data has added depth to engagement analysis. Sarkar et al. [16] demonstrated the utility of ECG data for emotion classification, which directly correlates with engagement levels. Gupta et al. [10] further extended this domain by combining facial features with physiological data such as heart rate variability, enabling a more holistic assessment of learner engagement. These efforts underline the importance of physiological signals in capturing subtle, non-visible aspects of engagement.

To overcome the limitations of single-modal approaches, researchers have increasingly focused on multimodal fusion techniques. Xie et al. [8] and Mehta et al. [9] explored early and late fusion strategies to integrate visual and physiological data streams. Early fusion combines raw features from multiple modalities, offering a unified feature representation, while late fusion integrates modality-specific predictions to enhance decision-making. These techniques have proven effective in capturing nuanced behavioral patterns and improving the robustness of engagement detection in complex environments.

Recent advancements in architecture design have further improved engagement detection. Vedernikov et al. [17] and Dubbaka et al. [18] refined deep learning models to handle diverse educational settings. Copur et al. [19] and Singh et al. [20] extended engagement analysis into informal and digital environments, emphasizing the adaptability of these systems.

Machine learning models continue to play a pivotal role in engagement analysis. Sherly et al. [21], Hasnine et al. [22], and Sharma et al. [23] implemented various machine learning techniques to address challenges such as data imbalance and computational efficiency. Ensemble methods, including random forests and boosting algorithms, have been particularly effective in improving prediction accuracy by combining multiple weak learners into a robust model.

Real-time engagement detection has been a critical focus area. Chen et al. [3] and Lee et al. [24] addressed the challenges of deploying engagement detection systems in real-time, emphasizing the importance of lightweight models that can operate efficiently under varied conditions. Gupta et al. [25] proposed deep learning-based systems tailored for dynamic environments, showcasing the potential of these models to adapt to changing engagement levels.

The synthesis of visual and physiological data has led to groundbreaking systems like VisioPhysioENet. Yang et al. [26]

and Liao et al. [27] demonstrated the effectiveness of combining modalities for nuanced behavior analysis. Savchenko et al. [28] introduced streamlined CNN architectures optimized for engagement detection, while Abedi et al. [29] highlighted the capabilities of engagement analysis for real-time applications.

Building on these advancements, our research addresses critical gaps in engagement detection. We propose VisioPhysioENet, a novel multimodal system that incorporates advanced fusion techniques, including early and late fusion, to seamlessly integrate visual and physiological data. The system converts unstructured input data (video frames) into structured numeric tabular data, achieving dimensionality reduction where traditional machine learning models excel. [30] It is optimized for lightweight deployment, ensuring minimal computational overhead while maintaining high accuracy. By focusing on real-time processing and scalability, VisioPhysioENet provides robust engagement detection across diverse educational and informal learning environments.

III. VISIOPHYSIOENET

The architecture of the proposed system, VisioPhysioENet, is shown in Fig. 1 and described below. The theory for feature extraction and fusion is presented as follows.

A. Visual Feature Extraction Phase

The visual feature extraction model operates at two levels, denoted as \mathcal{L}_i^V , to extract features from videos (V) by processing frames (f_i) sequentially. The first level, \mathcal{L}_1^V , involves extracting direct features as facial landmarks (p_1 to p_{68}) including eye metrics points (ε) and head position estimation points (h). These features are identified using the 68-FLM landmarks detection model provided by the Dlib library. This model has been pre-trained on the i-BUG-300-W dataset where it achieved a (Normalized Root Mean Square Error (NRMSE) of 0.209. [31]

$$\forall i \{ (f_i \in V) \{ \mathcal{L}_1(f_i) \} \} \xrightarrow{[FLM]} \{ \{ p_1 - p_{68} \}; \{ h \}; \{ \varepsilon \} \} \quad (1)$$

The \mathcal{L}_1^V also involves extracting numerical features from Eq (1)'s data. This includes the Eye Aspect Ratio (ξ) and parameters related to the position of the head [HP], such as pitch θ_x , yaw θ_y , and roll θ_z .

EAR measures the ratio of vertical to horizontal distances between specific eye points. While pitch measures the up-and-down movement of the head, yaw measures the left-to-right rotation of the head, and roll measures the side-to-side tilt of the head. The EAR (ξ) is calculated using the facial landmark points of both the left (ξ_L) and right eyes (ξ_R), and then their mean is taken.

$$\xi \xleftarrow{\sum/2} \begin{cases} \xi_L = \frac{\|p_{37}-p_{41}\| + \|p_{38}-p_{40}\|}{2\|p_{36}-p_{39}\|} \\ \xi_R = \frac{\|p_{43}-p_{47}\| + \|p_{44}-p_{46}\|}{2\|p_{42}-p_{45}\|} \end{cases} \quad (2)$$

where $\xleftarrow{\sum/2}$ denotes the computation of the mean and assignment operator. The numerator of these two equations is

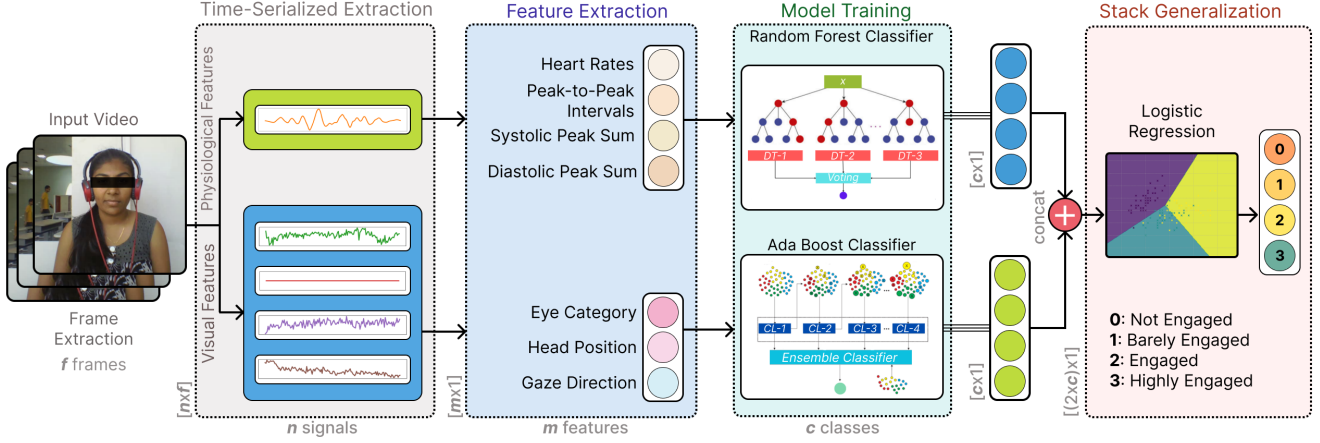


Fig. 1. Schematic architecture of VisioPhysioNet encompassing feature extraction modules for visual and physiological modalities and the fusion module.

the distance between the vertical eye landmarks while the denominator is the distance between horizontal eye landmarks. When the eye is open, the EAR is practically constant, but when the eye blinks, it quickly drops to zero. The higher the EAR, the wider the eye is open [32]. For head pose (HP) estimation, specific facial landmarks, such as nose tip, chin, corners of the eye, and mouth corners are used. The process assumes no camera distortions during focal length estimation. The rotation vector $\{\mathbf{RV}_{[i,j]}^{3 \times 1}\}$, describing the object's orientation relative to the camera, is computed using the `solvePNP` function specifically utilizing its iterative approach. The iterative method leverages the Levenberg-Marquardt algorithm [33] [34], a robust optimization technique that utilizes the advantages of both gradient descent and Gauss-Newton methods [35].

The Levenberg-Marquardt algorithm is particularly well-suited for minimizing non-linear least squares problems, such as the reprojection error in pose estimation. Iteratively refining the camera pose parameters ensures convergence towards a local minimum, even in the presence of noise or suboptimal initial estimates. This combination of gradient descent's stability and the Gauss-Newton method's rapid convergence enables the iterative approach to achieve both precision and reliability.

The OpenCV first extracts the axis 'u' and angle θ from the rotation vector $\{\mathbf{RV}_{[i,j]}^{3 \times 1}\}$. It then constructs the skew-symmetric matrix K and calculates the R using the below formula.

$$R = I + \sin(\theta) \cdot K + (1 - \cos(\theta)) \cdot K^2 \quad (3)$$

The $\mathbf{RV}_{[i,j]}^{3 \times 1}$ is converted to a rotation matrix $\mathbf{RM}_{[i,j]}^{3 \times 3}$ using the Rodrigues formula.

$$\mathbf{RV}_{[i,j]}^{3 \times 1} \xrightarrow[\text{Rodrigues}]{R} \mathbf{RM}_{[i,j]}^{3 \times 3} \quad (4)$$

The $\mathbf{RM}_{[i,j]}^{3 \times 3}$ is then used to extract the Euler angles, as per the standard algorithm, to obtain the values of pitch θ_x , yaw θ_y , and roll θ_z .

The next level, i.e., \mathcal{L}_2^V , involves extracting categorical

variables such as eye gaze direction (φ), head position (\hat{h}), and eye openness category (ϵ) from the numerical variables derived in \mathcal{L}_1^V . Categorical features can capture distinct, non-continuous groups or categories, which often represent real-world concepts more accurately. This distinction can provide meaningful insights that might be lost if the data were treated as numerical. To calculate φ , the image center (\odot) and eye center (\otimes) have been used, as follows:

$$\varphi \leftarrow \begin{cases} \odot \leftarrow \left\{ \left(\frac{\text{Image Width}}{2}, \frac{\text{Image Height}}{2} \right) \right\} \\ \otimes \leftarrow \frac{\sum_{i=36}^{41} p_i}{\sum_{i=42}^{47} p_i} \end{cases} \quad (5)$$

The gaze direction (φ), computed based on the gaze vector consisting of horizontal (x) and vertical (y) components, indicates whether a person is looking left, right, up, down, or forward based on its values. \hat{h} , computed based on θ_x, θ_y , and θ_z , has 7 classes, including neutral, tilted, or turned in various directions. Eye openness (ϵ), measured by EAR (ξ), is categorized into three classes: fully open, partially closed, and closed. All categorical variables depend on thresholds determined experimentally for each variable.

B. Physiological Feature Extraction Phase

The second phase of feature extraction focuses on extracting the Blood Volume Pulse (BVP) signal from video frames to reflect cardiovascular activity using the Plane-Orthogonal-to-Skin (POS) method [36], a non-invasive technique for rPPG. This method capitalizes on subtle changes in skin color caused by blood flow to estimate the BVP signal.

The \mathcal{L}_1^P denotes the first level in extracting physiological features, which begins with extracting signals (S) by calculating the average RGB values from a specified region of interest (ROI) i.e. forehead [37] (\mathcal{R}_f) for the proposed model in each video frame. ROI is identified and extracted using the `face_recognition` [14] library for accurate localization in each

video frame.

$$\mathbf{S}_t = \frac{1}{N} \sum_{i=1}^N (R_i(t), G_i(t), B_i(t)) \quad (6)$$

where $R_i(t)$, $G_i(t)$, and $B_i(t)$ are the RGB values from the region of interest in the i^{th} video frame, and N is the total number of pixels in the (\mathbb{R}_f) .

The temporal normalization is then applied to the RGB values by dividing each color signal by its mean over a specific time window. This transformation emphasizes the pulsatile component, primarily captured in the green channel, which is most sensitive to blood flow changes. The normalized signals are calculated as:

$$R_{\text{norm}}(t) = \frac{R(t)}{\mu_R} \quad G_{\text{norm}}(t) = \frac{G(t)}{\mu_G} \quad B_{\text{norm}}(t) = \frac{B(t)}{\mu_B} \quad (7)$$

where μ_R , μ_G , and μ_B are the mean values of the $R(t)$, $G(t)$, and $B(t)$ signals over the time window, respectively. This process reduces noise and variations unrelated to the pulse signal, ensuring the output reflects pulsatile changes due to blood flow.

After normalization, the signal is projected onto a plane orthogonal to the skin tone vector using a transformation matrix. This matrix highlights the pulsatile component, mostly captured in the green channel, sensitive to blood flow changes. The projection is defined as:

$$\mathbf{S}_{\text{proj}}(t) = \mathbf{T} \cdot \mathbf{S}_{\text{norm}}(t) \quad (8)$$

$$\mathbf{S}_{\text{norm}}(t) = \begin{bmatrix} R_{\text{norm}}(t) \\ G_{\text{norm}}(t) \\ B_{\text{norm}}(t) \end{bmatrix} \quad (9)$$

This transformation emphasizes the pulsatile component, primarily captured in the green channel, which is most sensitive to changes in blood flow.

In the next step, refinement is performed by tuning the signal components based on their standard deviation (σ_S). This step enhances the accuracy of the BVP signal by minimizing noise and artifacts, such as motion or lighting changes. The refined signals are calculated as:

$$\mathbf{S}_{\text{refined}}(t) = \frac{\mathbf{S}_{\text{proj}}(t)}{\sigma_S} \quad (10)$$

where $\mathbf{S}_{\text{refined}}(t)$ is the refined signal, $\mathbf{S}_{\text{proj}}(t)$ is the signal's projection and σ_S is standard deviation.

After obtaining the BVP signal from \mathcal{L}_1^P , further in \mathcal{L}_2^P analysis is conducted to extract more physiological features. Then the BVP signal is detrended to remove long-term trends and, a band-pass filter is applied to isolate the heart rate frequency components from the $\tilde{B}(t)$.

$$\tilde{B}(t) = B(t) - \text{Trend}(B(t)) \quad || \quad B_{\text{filtered}}(t) = \mathcal{F}_{\text{BP}}(\tilde{B}(t)) \quad (11)$$

where $B(t)$ is the original BVP signal, and $\tilde{B}(t)$ is the detrended signal. \mathcal{F}_{BP} denotes the band-pass filter, and $B_{\text{filtered}}(t)$ is the filtered signal.

After extracting the BVP signal using the POS method, it is further processed to compute meaningful metrics such as heart rate, average peak-to-peak interval, and cumulative sums of systolic and diastolic peaks, providing insights into cardiovascular activity. The RR interval RR_i represents the time between consecutive detected heartbeats. The timestamps of the detected peaks are denoted as t_i and t_{i+1} , where i is the index of the peak. The RR interval for each pair of consecutive peaks is calculated as:

$$RR_i = t_{i+1} - t_i \quad \forall_{i=1}^{N-1}$$

where N is the total number of peaks detected in the signal. This gives the interval between each pair of consecutive heartbeats.

The mean RR interval, \overline{RR} , is the average of all RR intervals and represents the average time between heartbeats. The formula to calculate the mean RR interval is:

$$\overline{RR} = \frac{1}{N-1} \sum_{i=1}^{N-1} RR_i$$

where $N-1$ represents the number of RR intervals for N detected peaks, and RR_i represents the i -th RR interval.

The heart rate in beats per minute (BPM) can be derived from the mean RR interval. It is given by:

$$\text{BPM} = \frac{60}{\overline{RR}}$$

where \overline{RR} is the mean RR interval in seconds, and the factor of 60 converts the interval from seconds to minutes, giving the average heart rate in beats per minute.

The average peak-to-peak interval (PPI), which assesses heart rhythm regularity, is essentially the same as the mean RR interval. It is calculated as:

$$\text{PPI}_{\text{avg}} = \frac{1}{N-1} \sum_{i=1}^{N-1} RR_i$$

Since the PPI is the same as the mean RR interval, we have $\text{PPI}_{\text{avg}} = \overline{RR}$. This value reflects the regularity of the heartbeats during the analysis.

To assess cardiovascular activity, we calculate the cumulative sums of systolic and diastolic peaks. Let S_i and D_i represent the systolic and diastolic peaks at the i -th instance. The cumulative sums of systolic and diastolic peaks are given by:

$$CS_{\text{Sys}} = \sum_{i=1}^N S_i \quad \text{and} \quad CS_{\text{Dia}} = \sum_{i=1}^N D_i$$

where N is the total number of detected systolic and diastolic peaks, and S_i and D_i represent the values of the systolic and diastolic peaks at each instance.

The cumulative sums provide a measure of the overall cardiovascular activity, with CS_{Sys} reflecting the sum of systolic events and CS_{Dia} reflecting the sum of diastolic events during the signal period.

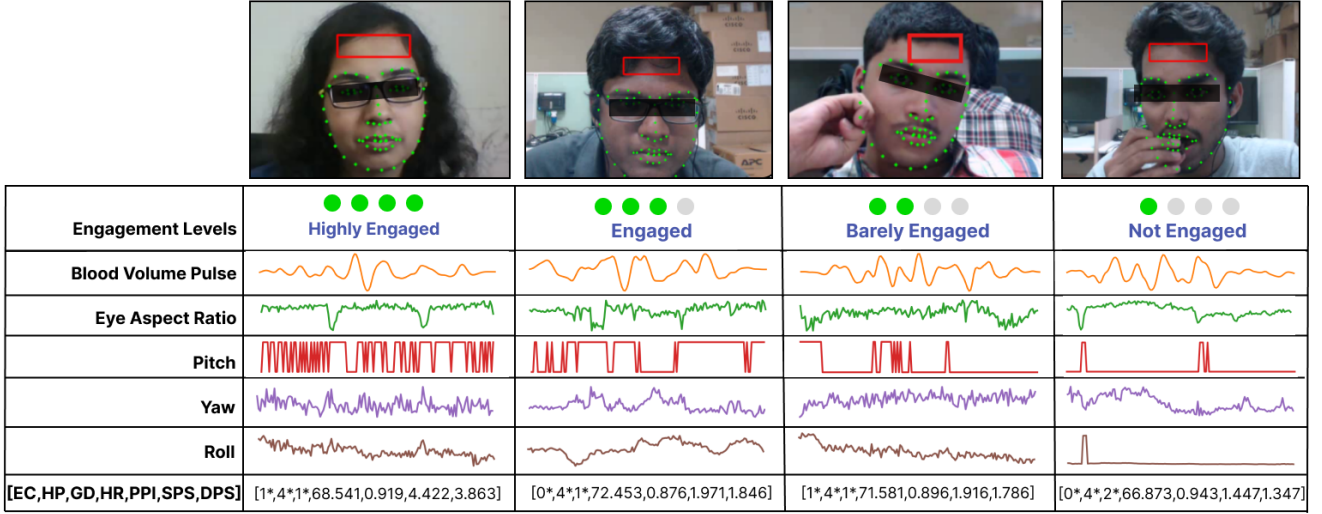


Fig. 2. Sample Results. Here, EC: Eye Category, HP: Head Position, GD: Gaze Direction, HR: Heart Rate, PPI: Peak-to-Peak Interval, SPS: Systolic Peak Sum, DPS: Diastolic Peak Sum; * represents categorical values while others are numeric values.

C. Multimodal Fusion Phase

In our proposed architecture, we implement a Late Fusion strategy to effectively integrate Visual and Physiological features for enhanced classification performance. The visual features extracted in section III-A \mathcal{L}_2^V are processed using AdaBoost Classifier [38], to compute the probability distribution, $P_{AB}(V)$.

$$P_{AB}(V) = \text{AdaBoost}(\{\varphi, h, \epsilon\}) \quad (12)$$

where $P_{AB}(V)$ is the probability distribution output from the AdaBoost classifier based on the visual features.

On the other hand, the Physiological features from \mathcal{L}_2^P computed in section III-B are used for assessing the subject's physiological responses using a Random Forest Classifier [39].

$$P_{RF}(P) = \text{RandFor}\{PPI_{avg}, CS_{Sys}, CS_{Dia}, HR_{trend}\} \quad (13)$$

where $P_{RF}(P)$ is the probability distribution output from the Random Forest classifier based on the physiological features.

In the final stage, a Late Fusion technique using stacked generalization [40] combines the probabilities P_{AB} and P_{RF} using a meta-classifier (logistic regression [41]), producing the final classification.

$$\hat{y} \leftarrow \arg \max \left\{ P_{\text{final}} = \text{MetaClassifier}(P_{AB}(V), P_{RF}(P)) \right\} \quad (14)$$

This Late Fusion approach allows our model to capitalize on the complementary strengths of AdaBoost and Random Forest, ensuring that both visual and physiological information is utilized to its full potential. The result is a more accurate and robust classification model that effectively synthesizes multimodal data to make well-informed predictions.

IV. EXPERIMENTAL RESULTS

A. Setup

1) *Dataset and Implementation:* The proposed system was evaluated using the train and test subsets from the DAiSEE dataset [15], which includes 9,068 videos from 112 adults, annotated by human experts. The model training used an 80-20 train-test split and 10-fold cross-validation, conducted on an Intel(R) Core(TM) i7-7700, 3.70 GHz and Nvidia RTX 2070 GPU.

2) *Models:* To establish a comprehensive understanding of the proposed system's efficiency, three distinct baseline models were developed based on the insights from ablation studies discussed in Section IV-D.

- *Baseline 1:* Utilizes visual features, including eye category, head positioning, and gaze direction, to analyze visual cues from the data.
- *Baseline 2:* Processes physiological signals such as heart rate and the cumulative sum of systolic and diastolic peaks, focusing on the physical aspects of the dataset.
- *Baseline 3:* Combines both visual and physiological modalities through an early fusion technique, serving as a foundational comparison for the proposed system which applies a more sophisticated late fusion approach for modality integration.

B. Quantitative Results

Our system's performance, as shown in Table I, underscores its superiority over existing approaches by incorporating a novel integration of visual and physiological data. Notably, it outperforms the model by Vedernikov et al. [42], which also combines these modalities but with less efficacy. The proposed system achieves an accuracy improvement of 8.6% over this model, demonstrating the effectiveness of the late fusion approach in handling multimodal data. This significant

improvement in performance highlights the potential of our methodology to advance research in the field of multimodal systems, setting a new benchmark for future studies.

TABLE I

RESULTS' COMPARISON WITH STATE-OF-THE-ART. HERE, 'V,' 'P' AND 'ACC' DENOTE VISUAL & PHYSIOLOGICAL MODALITIES AND ACCURACY

Model	Modality	Acc
InceptionNet Video Level [15]	V	46.40%
InceptionNet Frame Level [15]	V	47.10%
Class-Balanced 3D CNN [43]	V	52.35%
ResNet + Temporal Conv Net [6]	V	53.70%
Unsupervised Behavior & rPPG [42]	V+P	54.49%
Long-Term Recurrent Conv Net [15]	V	57.90%
Deep Spatiotemporal Net [27]	V	58.84%
C3D + TCN [6]	V	59.97%
ResNet + LSTM [6]	V	61.15%
VisioPhysioENet	V+P	63.09%
ResNet + TCN [6]	V	63.90%
Ordinal TCN [44]	V	67.40%

Despite not achieving the highest accuracy, VisioPhysioENet stands out by leveraging both physiological and visual data, providing a richer, more nuanced understanding of engagement. It outperforms the only other multimodal model by 8.6%, demonstrating its superior ability to integrate these data types. The unique features of VisioPhysioENet, such as advanced feature extraction and fusion techniques, enhance its utility in real-world educational settings. Additionally, the robustness and generalizability of the model suggest it can effectively handle variations and imbalances across different datasets, making it a valuable tool for practical applications.

C. Qualitative Results

Fig. 2 shows sample results. Visual metrics like head position is influenced by pitch, yaw, and roll; eye gaze direction by landmarks while eye openness category from Eye-Aspect Ratio (EAR). Physiological metrics, derived from the BVP signal, include heart-rate (HR) and peak-to-peak (P2P) interval, where crests and troughs indicate systolic and diastolic peaks, respectively.

D. Ablation Studies

1) *Choice of Appropriate Fusion Approach:* The following studies have been carried out to select the appropriate architecture for the proposed model.

Table II presents our fusion approaches, highlighting how stacked generalization effectively harnesses the strengths of both AdaBoost and Random Forest. By incorporating error correction from these models and enhancing robustness through a logistic regression meta-classifier, this approach optimizes the integration of diverse feature sets. The result is a significantly improved engagement prediction accuracy, reaching 63.09%, which outperforms all baselines. This superior performance underscores the efficacy of combining multiple learning strategies to refine predictive accuracy in complex datasets.

TABLE II
ABLATION STUDIES (CHOICE OF FUSION APPROACH). HERE, 'V' AND 'P' REPRESENT VISUAL AND PHYSIOLOGICAL MODALITIES.

Model	Modality	Fusion Strategy	Acc
Baseline 1	V	–	43.03%
Baseline 2	P	–	55.25%
Baseline 3	V+P	Early Fusion	51.50%
Proposed	V+P	Late Fusion	63.09%

2) *Choice of Machine Learning Models:* Tables III and IV outline the machine learning models selected for visual and physiological modalities. The AdaBoost Classifier, achieving an accuracy of 43.03% for visual features, is chosen for its ability to enhance performance by focusing on difficult cases in complex visual data, such as variations in lighting and expression. In contrast, the Random Forest Classifier, which attains a higher accuracy of 55.25% for physiological features, is utilized due to its robustness in handling multivariate data and the feature selection capabilities essential for physiological signals such as heart rate and blood pressure peaks.

TABLE III
CHOICE OF ML MODELS FOR VISUAL MODALITY

Model	Accuracy
K-Nearest Neighbors Classifier	39.66%
Gradient Boost Classifier	42.77%
Support Vector Classifier	42.77%
Random Forest Classifier	42.86%
Decision Tree Classifier	42.95%
Ada Boost Classifier	43.03%

TABLE IV
CHOICE OF ML MODELS FOR PHYSIOLOGICAL MODALITY.

Model	Accuracy
Ada Boost Classifier	44.54%
Support Vector Classifier	46.76%
Decision Tree Classifier	51.67%
K-Nearest Neighbors Classifier	51.91%
Gradient Boost Classifier	54.48%
Random Forest	55.25%

3) *Computational requirements analysis:* Pre-extracting relevant features from raw video frames allows for parallel processing. Sequential task execution often results in idle processor time, reducing overall system efficiency. To address this, we implemented the ThreadPoolExecutor [45], which facilitates parallel processing by allowing multiple tasks to run concurrently across different threads. This approach not only optimizes CPU usage by reducing idle time but also enhances throughput. Table V details the performance improvements achieved with parallel processing techniques compared to

traditional sequential methods, highlighting significant gains in processing speed and efficiency.

TABLE V
COMPARISON OF SEQUENTIAL (ST) AND THREADPOOLEXECUTOR (TPE)
TIMES IN SECONDS.

Batch Size	1	2	4	8	16	32	64
ST	7.4s	14.1s	27.2s	55.8s	109.7s	255.6s	732.6s
TPE Time	7.0s	8.8s	12.4s	21.9s	44.9s	100.0s	293.0s

E. Discussion

The development of VisioPhysioENet introduces a novel approach in the area of multimodal engagement detection by leveraging both visual and physiological data streams. This innovative integration provides a more nuanced understanding of learner engagement, significantly improving both accuracy and robustness. With an accuracy of 63.09% on the DAiSEE dataset, VisioPhysioENet surpasses existing unimodal and multimodal methods. A distinct advantage of VisioPhysioENet lies in its advanced feature extraction techniques and efficient data integration strategy, which effectively handles real-world educational environments. The use of Dlib and OpenCV for visual feature extraction and the POS method for physiological signal analysis also ensures high performance with minimal computational overhead, making the system highly suitable for real-time applications that demand rapid and reliable engagement detection.

As shown in Tables III, II, and IV, the visual modality achieves 43.90% accuracy, while physiological signals alone yield 55.25%. By integrating these two streams, VisioPhysioENet attains 63.09%, illustrating how the multimodal approach captures complementary information often overlooked in unimodal systems. This combination leads to more robust performance and offers deeper insights into learners' engagement states. Such synergy is particularly valuable in diverse educational settings where variations in gaze, facial expressions, and physiological responses contribute to the overall engagement profile.

Despite these strengths, the system faces challenges, especially regarding sensitivity to environmental variables such as lighting and motion artifacts. These factors can complicate data collection and introduce noise. Consequently, further refinement and additional testing are needed to ensure greater robustness across diverse populations and scenarios. Moreover, integrating physiological signals adds complexities in data capture and interpretation—small changes in emotional or physical state can alter physiological readings. Improved algorithms are crucial to distinguish between the variations that genuinely indicate engagement and those arising from unrelated factors.

VisioPhysioENet's strong performance in utilizing multimodal (visual and physiological) data suggests its applicability in various applications. For example, in education, it can monitor student engagement levels, enhancing instructional strategies and ultimately improving learning outcomes [23]. In corporate training, this approach could strengthen employee

learning retention [46]. Healthcare is another promising domain: by gauging patients' understanding of treatment plans, clinicians can adjust patient education [2]. In advertisement, marketing, and consumer research, insights into consumer responses to media and advertising can be gleaned using this system [47]. Additionally, virtual events and conferences can benefit, as real-time feedback can inform dynamic content adjustments to heighten attendee engagement [42].

V. CONCLUSION AND FUTURE DIRECTIONS

VisioPhysioENet, a novel multimodal system that integrates visual cues and physiological signals, has been proposed to effectively detect learner engagement. Achieving a commendable accuracy of 63.09% on the DAiSEE dataset, it outperforms several state-of-the-art methods. This balance of accuracy and efficiency makes it a robust solution for real-world applications, especially suitable for dynamic environments.

Future enhancements will focus on improving scalability and robustness across diverse user groups and environments. This will include integrating additional modalities, such as audio cues and contextual data, to enrich the system's understanding of learner engagement. Efforts will also aim to adapt the system for varied educational contexts, such as online learning platforms, virtual classrooms, and hybrid learning setups, ensuring its real-world adaptability and applicability in personalized learning experiences. Through these developments, VisioPhysioENet aims to become a versatile tool to advance intelligent educational technologies.

REFERENCES

- [1] I. Alkabbany, A. Ali, A. Farag, I. Bennett, M. Ghanoum, and A. Farag, "Measuring student engagement level using facial information," in *2019 IEEE International Conference on Image Processing (ICIP)*. IEEE, 2019, pp. 3337–3341.
- [2] P. Kumar, A. Vedernikov, and X. Li, "Measuring Non-Typical Emotions for Mental Health: A Survey of Computational Approaches," *arXiv preprint arXiv:2403.08824*, 2024, Accessed on 30.08.2024.
- [3] X. Chen, L. Niu, A. Veeraraghavan, and A. Sabharwal, "Faceengage: Robust estimation of gameplay engagement from user-contributed (youtube) videos," *IEEE Transactions on Affective Computing*, vol. 13, no. 2, pp. 651–665, 2019.
- [4] P. Kumar, S. Malik, B. Raman, and X. Li, "VISTANet: Visual Spoken Textual Additive Net for Interpretable Multimodal Emotion Recognition," *arXiv preprint arXiv:2208.11450*, pp. arXiv–2208, 2022, accessed 05 Sep 2024.
- [5] Ö. Sümer, P. Goldberg, S. D'Mello, P. Gerjets, U. Trautwein, and E. Kasneci, "Multimodal engagement analysis from facial videos in the classroom," *IEEE Transactions on Affective Computing*, vol. 14, no. 2, pp. 1012–1027, 2021.
- [6] A. Abedi and S. S. Khan, "Improving State-Of-The-Art In Detecting Student Engagement With ResNet and TCN Hybrid Network," in *2021 18th Conference on Robots and Vision (CRV)*. IEEE, 2021, pp. 151–157.
- [7] T. Selim, I. Elkabani, and M. A. Abdou, "Students engagement level detection in online e-learning using hybrid efficientnetb7 together with tcn, lstm, and bi-lstm," *IEEE Access*, vol. 10, pp. 99 573–99 583, 2022.
- [8] N. Xie, Z. Liu, Z. Li, W. Pang, and B. Lu, "Student engagement detection in online environment using computer vision and multi-dimensional feature fusion," *Multimedia Systems*, vol. 29, no. 6, pp. 3559–3577, 2023.
- [9] N. K. Mehta, S. S. Prasad, S. Saurav, R. Saini, and S. Singh, "Three-dimensional densenet self-attention neural network for automatic detection of student's engagement," *Applied Intelligence*, vol. 52, no. 12, pp. 13 803–13 823, 2022.

- [10] S. Gupta, P. Kumar, and R. Tekchandani, "A multimodal facial cues based engagement detection system in e-learning context using deep learning approach," *Multimedia Tools and Applications*, vol. 82, no. 18, pp. 28 589–28 615, 2023.
- [11] D. E. King. (2016) DLIB Models. <https://github.com/davisking/dlib-models>. Accessed on 30.08.2024.
- [12] G. Bradski, "Opencv (open source computer vision library)," 1999.
- [13] A. Ghosh, A. Finkelstein, P. Matus, and S. Muthukumar, "Remote photoplethysmographic imaging using ambient light," *IEEE Transactions on Biomedical Engineering*, vol. 62, no. 7, pp. 1592–1601, 2015.
- [14] A. Ageitgey, "face_recognition," 2017, accessed: 2024-01-03. [Online]. Available: https://github.com/ageitgey/face_recognition
- [15] A. Gupta, A. D'Cunha *et al.*, "DAiSEE: Towards User Engagement Recognition in the Wild," *arXiv preprint arXiv:1609.01885*, 2016.
- [16] P. Sarkar and A. Etemad, "Self-supervised ecg representation learning for emotion recognition," *IEEE Transactions on Affective Computing*, vol. 13, no. 3, pp. 1541–1554, 2020.
- [17] A. Vedernikov, P. Kumar, H. Chen, T. Seppänen, and X. Li, "Tcct-net: Two-stream network architecture for fast and efficient engagement estimation via behavioral feature signals," in *Proceedings of the IEEE/CVF Conference on Computer Vision and Pattern Recognition (CVPR)*, 2024, pp. 4723–4732.
- [18] A. Dubbaka and A. Gopalan, "Detecting learner engagement in moocs using automatic facial expression recognition," in *2020 IEEE Global Engineering Education Conference (EDUCON)*. IEEE, 2020, pp. 447–456.
- [19] O. Copur, M. Nakip, S. Scardapane, and J. Slowack, "Engagement detection with multi-task training in e-learning environments," in *International Conference on Image Analysis and Processing*. Springer, 2022, pp. 411–422.
- [20] M. Singh, X. Hoque, D. Zeng, Y. Wang, K. Ikeda, and A. Dhall, "Do i have your attention: A large scale engagement prediction dataset and baselines," in *Proceedings of the 25th International Conference on Multimodal Interaction*, 2023, pp. 174–182.
- [21] E. Sherly *et al.*, "Fostering learning with facial insights: Geometrical approach to real-time learner engagement detection," in *2024 IEEE 9th International Conference for Convergence in Technology (I2CT)*. IEEE, 2024, pp. 1–6.
- [22] M. N. Hasnine, H. T. Bui, T. T. T. Tran, H. T. Nguyen, G. Akçapınar, and H. Ueda, "Students' emotion extraction and visualization for engagement detection in online learning," *Procedia Computer Science*, vol. 192, pp. 3423–3431, 2021.
- [23] P. Sharma, S. Joshi, S. Gautam, S. Maharjan, S. R. Khanal, M. C. Reis, J. Barroso, and V. M. de Jesus Filipe, "Student engagement detection using emotion analysis, eye tracking and head movement with machine learning," in *International Conference on Technology and Innovation in Learning, Teaching and Education*. Springer, 2022, pp. 52–68.
- [24] T. Lee, D. Kim, S. Park, D. Kim, and S.-J. Lee, "Predicting mind-wandering with facial videos in online lectures," in *Proceedings of the IEEE/CVF Conference on Computer Vision and Pattern Recognition*, 2022, pp. 2104–2113.
- [25] S. Gupta, P. Kumar, and R. K. Tekchandani, "Facial emotion recognition based real-time learner engagement detection system in online learning context using deep learning models," *Multimedia Tools and Applications*, vol. 82, no. 8, pp. 11 365–11 394, 2023.
- [26] C. Yang, K. Wang, P. Q. Chen, M. M. Cheung, Y. Zhang, E. Y. Fu, and G. Ngai, "Multimediate 2023: Engagement level detection using audio and video features," in *Proceedings of the 31st ACM International Conference on Multimedia*, 2023, pp. 9601–9605.
- [27] J. Liao, Y. Liang *et al.*, "Deep Facial Spatiotemporal Network for Engagement Prediction in Online Learning," *Applied Intelligence*, vol. 51, pp. 6609–6621, 2021.
- [28] A. V. Savchenko, L. V. Savchenko, and I. Makarov, "Classifying emotions and engagement in online learning based on a single facial expression recognition neural network," *IEEE Transactions on Affective Computing*, vol. 13, no. 4, pp. 2132–2143, 2022.
- [29] A. Abedi and S. S. Khan, "Engagement measurement based on facial landmarks and spatial-temporal graph convolutional networks," *arXiv preprint arXiv:2403.17175*, 2024.
- [30] L. Grinsztajn, E. Oyallon, and G. Varoquaux, "Why do tree-based models still outperform deep learning on typical tabular data?" *Advances in neural information processing systems*, vol. 35, pp. 507–520, 2022.
- [31] O. Golob, "Analysis of face detection, face landmarking, and face recognition performance with masked face images," 2022. [Online]. Available: <https://arxiv.org/abs/2207.06478>
- [32] T. Soukupová and J. Cech, "Real-time eye blink detection using facial landmarks," 2016. [Online]. Available: <https://api.semanticscholar.org/CorpusID:21124316>
- [33] K. Levenberg, "A method for the solution of certain non – linear problems in least squares," *Quarterly of Applied Mathematics*, vol. 2, pp. 164–168, 1944. [Online]. Available: <https://api.semanticscholar.org/CorpusID:124308544>
- [34] D. W. Marquardt, "An algorithm for least-squares estimation of nonlinear parameters," *Journal of the Society for Industrial and Applied Mathematics*, vol. 11, no. 2, pp. 431–441, 1963. [Online]. Available: <http://www.jstor.org/stable/2098941>
- [35] Y. Wang, "Gauss–Newton method," *Wiley Interdisciplinary Reviews: Computational Statistics*, vol. 4, no. 4, pp. 415–420, 2012.
- [36] W. Wang, A. C. den Brinker, S. Stuijk, and G. de Haan, "Algorithmic principles of remote ppg," *IEEE Transactions on Biomedical Engineering*, vol. 64, no. 7, pp. 1479–1491, 2017.
- [37] S. Kwon, J. Kim, D. Lee, and K. Park, "Roi analysis for remote photoplethysmography on facial video," in *2015 37th Annual International Conference of the IEEE Engineering in Medicine and Biology Society (EMBC)*, 2015, pp. 4938–4941.
- [38] Y. Freund, R. Schapire, and N. Abe, "A short introduction to boosting," *Journal-Japanese Society For Artificial Intelligence*, vol. 14, no. 771–780, p. 1612, 1999.
- [39] L. Breiman, "Random forests," *Machine learning*, vol. 45, pp. 5–32, 2001.
- [40] D. H. Wolpert, "Stacked generalization," *Neural networks*, vol. 5, no. 2, pp. 241–259, 1992.
- [41] D. R. Cox, "The regression analysis of binary sequences," *Journal of the Royal Statistical Society Series B: Statistical Methodology*, vol. 20, no. 2, pp. 215–232, 1958.
- [42] A. Vedernikov, Z. Sun, V.-L. Kykyri, M. Pohjola, M. Nokia, and X. Li, "Analyzing Participants' Engagement during Online Meetings Using Unsupervised Remote Photoplethysmography with Behavioral Features," in *Proceedings of the IEEE/CVF Conference on Computer Vision and Pattern Recognition Workshops (CVPRw)*, 2024, pp. 389–399.
- [43] H. Zhang, X. Xiao, T. Huang *et al.*, "An Novel End-to-End Network for Automatic Student Engagement Recognition," 2019, Conference paper, p. 342 – 345.
- [44] A. Abedi and S. S. Khan, "Affect-driven ordinal engagement measurement from video," *Multimedia Tools and Applications*, vol. 83, no. 8, pp. 24 899–24 918, 2024.
- [45] E. J. New, T. Model, R. Veen, and D. Vlijmincx, "Virtual Threads, Structured Concurrency, and Scoped Values."
- [46] C. Ma, C. K. M. Lee, J. Du, Q. Li, and R. Gravina, "Work engagement recognition in smart office," *Procedia Computer Science*, vol. 200, pp. 451–460, 2022.
- [47] S. P. John and R. De'Villiers, "Elaboration of marketing communication through visual media: An empirical analysis," *Journal of Retailing and Consumer Services*, vol. 54, p. 102052.